Silicon Kerr Effect Electro-optic Switch

Deepak V. Simili and Michael Cada
Department of Electrical and Computer Engineering, Dalhousie University, 1459 Oxford Street, Halifax, Canada

1 RESEARCH PROBLEM

The research problem that we are investigating deals with designing and testing an ultrafast silicon electro-optic switch for integrated-optic applications that employs the Kerr effect. Silicon photonics for optical interconnects offers a possibility to provide a low cost, mass manufacturable solution for data communication applications such as data centers, high performance computing, mobile devices (cell phones or tablets) to server interconnects, and desktop computers (Reed G.T et. al., 2010). A switch or a modulator is one of the building blocks in an integrated-optic data transmitter connected to a fiber-optic channel. In order to better utilize the THz bandwidth capabilities of fiber optic channels and to meet increasing bandwidth demands of future communication networks, it is highly desired to develop optical switches with modulation bandwidths in the range of 100 GHz and higher.

In this paper we address the problem of optimizing the ring resonator structure for the Kerr effect switch considered in previous work (Cada, 2011, Simili et. al., 2013) in order to achieve bandwidth performance in the range of 100 GHz or higher. An analysis of the key performance indicators of the switch is also presented.

2 OUTLINE OF OBJECTIVES

The desired characteristics for the electro-optic switch are as follows:

- Modulation bandwidth in the range of 100 GHz or higher.
- Low switching voltage on the order of a few volts.
- A Silicon-based device as silicon is widely used in the electronics industry and is compatible with the CMOS fabrication technique.
- Operating at the telecommunication wavelength of 1.55 micrometers.
- Compact size with a device footprint in the range of $10^2\ \mu m^2$ or lower.
- Average switching energy lower than 10 pJ/bit with a target of 10 fJ/bit.
- Overcome coupling losses due to polarization dependence.

The above mentioned objectives are based on a review of silicon-based electro-optic modulators present in the literature, which are discussed in the next section.

3 STATE OF THE ART

The most commonly used electro-optic effect to achieve modulation in silicon devices has been the plasma dispersion effect. This is because electric field effects based on electro-refraction such as the Pockels effect do not exist in silicon while the Kerr effect induces a small refractive index change $\Delta n = 10^{-6}$, for an applied electric field of 10^7 V/m (Soref et. al., 1987) at 1.55 micrometer wavelength to be useful for integrated-optic applications. Electric field effects in silicon, based on electro-absorption such as the Franz-Keldysh effect also induce a low refractive index change ($\Delta n = 1.5 \times 10^{-6},\ E = 10^7 V/m$) at 1.55 micrometers (Soref et. al., 1987) to be useful. For device applications a Δn of the order of 10^{-4} or greater is desired also to avoid a danger of an electrical breakdown of the medium. For intrinsic silicon at room temperature, the dielectric breakdown field is of the order of 3×10^7 V/m (Kim, 2010).

The plasma dispersion effect is based on a change in the free carrier concentration of silicon to induce a change in the absorption spectrum and therefore a change in the refractive index. The change in the refractive index of silicon was computed through experimentally obtained absorption spectrum in (Soref et. al., 1987). A refractive index change of the order of 10^{-3} was obtained for free carrier (electrons) concentration change of $10^{18}/cm^3$ at 1.55 micrometer wavelength. The different mechanisms used to achieve the plasma dispersion effect in the medium

V. Simili D. and Cada M..
Silicon Kerr Effect Electro-optic Switch.

through which light is propagating are carrier accumulation, carrier injection and carrier depletion.

In the carrier injection technique, electrons and holes are injected into an intrinsic waveguide region. The structure used is a p-i-n junction diode. The injection of electrons and holes into the waveguide region is controlled by changing the voltage applied to the highly doped p and n regions of the structure. The charge transport mechanism is based on carrier diffusion. The switch off time for the device would depend on the electron-hole recombination lifetime for silicon which is 100 ns for n-type silicon at temperature of 300 K (Saleh et. al., 2007). An example of a top performing modulator employing this technique uses a micro ring resonator structure to achieve speeds of 12.5 Gbps with a high extinction ratio greater than 9 dB at a modulation voltage of approximately 4 V (Xu et. al., 2007).

In the carrier accumulation technique, mobile carriers are diffused into the intrinsic waveguide region. The concentration of mobile carriers in the waveguide region is controlled by adjusting the potential of the doped regions. The intrinsic waveguide region is split into two halves separated by an insulator region so the mobile carriers begin to accumulate on both sides of the insulator to form a capacitor structure. This type of structure would avoid the slow recombination process of the diffused mobile carriers. The first implementation of this technique reported a bandwidth in the neighborhood of 1-2 GHz with an extinction ratio greater than 16 dB and a device phase efficiency ($V_\pi L$) of approximately 8 V.cm (Liu et. al., 2004). Subsequent optimizations to this technique reported 10 GHz bandwidth with 3.8 dB extinction ratio and a better $V_\pi L$ of 3.3 V.cm (Liao et. al., 2005).

In the carrier depletion technique, the silicon waveguide is a lightly doped p-n junction. The width of this depletion layer is controlled by reverse biasing the structure and therefore carrier concentration experienced by the propagating light in the waveguide is changed. This technique reported the highest bandwidth of 30 GHz, with an extinction ratio of 1.1 dB and a $V_\pi L$ of 4 V.cm (Liao et. al., 2007). The carrier transport mechanism in this case is carrier drift which is faster than the carrier diffusion used in previous techniques.

The main drawback of the plasma dispersion effect is that it relies on carrier transport phenomena of carrier drift or carrier diffusion for which the response times are at best in the range of picoseconds. Therefore this effect is not suitable for the design of electro-optic modulators with desired modulation speeds over 100 GHz.

4 METHODOLOGY

The general methodology in the design and development of a silicon-based electro-optic switch is selecting a silicon-based material with useful material properties for use with an ultrafast electro-optic effect. This is followed by using the material and the effect in a suitable structure to obtain a measure of performance parameters for the switch.

The material chosen as an optical medium for the silicon-based electro-optic switch is silicon nanocrystals in silica ($Si-nc/SiO_2$). It has a third-order nonlinear susceptibility ($\chi^{(3)}$) of $2\times10^{-18}m^2/V^2$ and $3.8\times10^{-19}\,m^2/V^2$ at a wavelength of 1.55 micrometers for LPCVD and PECVD deposition methods, respectively (Cada, 2008). These values are at least one order of magnitude greater than that of bulk silicon and silica glass (Cada, 2008). $Si-nc/SiO_2$ fabricated through the PECVD technique has a better material nonlinear figure of merit ($\frac{3\chi^{(3)}}{4\varepsilon_0 cn^2\beta_2\lambda}$) of 0.649 compared to that of silicon's 0.495 at the wavelength of 1.55 micrometers (Cada, 2008). This makes $Si-nc/SiO_2$ more suitable than silicon to be used with nonlinear effects such as the Kerr effect. $Si-nc/SiO_2$ can be mass manufactured through LPCVD and PECVD techniques, so the device would be CMOS compatible.

The physical effect chosen for the design analysis of a silicon-based electro-optic switch is the Kerr effect, which exists in all materials. It is a pure electric field-effect that depends on $\chi^{(3)}$ of the material, where the refractive index of the medium changes with a square of an applied electric field. It is inherently ultrafast as it depends on displacement of the electron cloud due to an applied electric field with response times on the order of 10^{-16} s for non-resonant conditions (Boyd, 2008). The induced refractive index change due to the Kerr effect (Δn) for a fully applied electric field is (Cada et. al., 2008)

$$\Delta n = \frac{3\chi^{(3)}E^2}{2n_L} \quad (1)$$

For an applied electric field E of 1V/100nm, a useful Δn of 1.76×10^{-4} is obtained for $Si-nc/SiO_2$, which can be considered as the dominant factor for the induced refractive index change in the medium. The induced refractive index change due to the optical Kerr effect ($\Delta n = n_2 I$) is at least 2 orders of magnitude smaller than the electric Kerr effect for low optical powers (1mW or less) with a waveguide

cross section of 0.1 μm^2. It has been experimentally observed that the ultrafast optical Kerr effect which is also based on $\chi^{(3)}$, dominates slow free carrier effects such as the two photon absorption at telecom wavelengths of 1550 nm in silicon nanocrystals (Martinez et. al., 2010). Therefore one can consider the pure electric field Kerr effect as the dominant effect compared to optical Kerr effect and slow free carrier effects in determining the refractive index changes of the medium.

5 EXPECTED OUTCOME

In this section we describe the optimization performed on a ring resonator structure for a Kerr switch and the analysis of key performance parameters of the Kerr switch. A ring resonator's transmission output is highly sensitive to the resonant wavelength of the ring structure. It is compact and has a size in the range of micrometers, which is suitable for integrated optic applications.

The criteria for choosing the ring resonator structure are that it should have a low cavity photon lifetime (around 1 ps or lower) to ensure a high maximum modulation bandwidth (100 GHz or higher) and there should be experimental data available on a ring resonator structure. One such ring resonator structure is the slot waveguide ring resonator described in (Xu et. al., 2004). This ring resonator has a diameter of 20 micrometers and the separation distance between the slot regions of the straight slot waveguide and the slot ring resonator is 1 micrometer. The Q-factor of the ring resonator is around 1000 at a wavelength of 1.55 micrometers in the experimentally obtained transmission spectrum

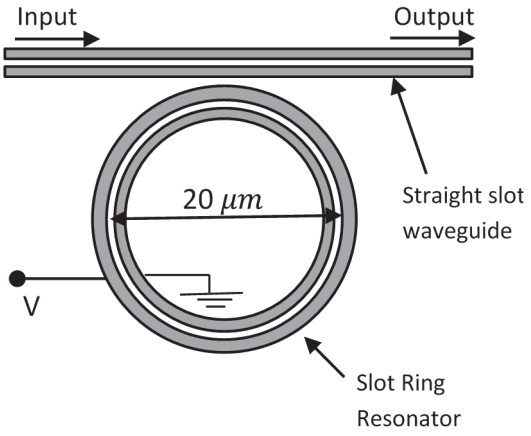

Figure 1: Schematic of the ring resonator structure for the Kerr switch.

(Xu et. al., 2004). This yields the structure's cavity photon lifetime of 0.822 ps. The layout of the considered ring resonator structure for the Kerr switch is shown in Figure 1.

We simulated the transmission resonance dip in the 1.55 micrometer regime of the measured transmission spectrum in the considered ring resonator.

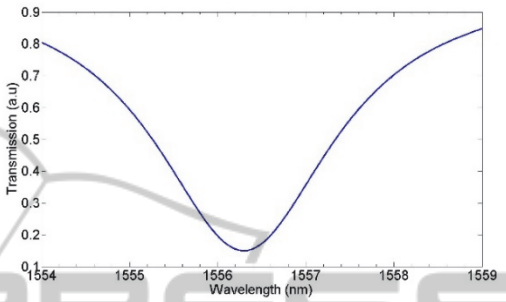

Figure 2: Transmission spectrum for the coupled slot ring resonator.

Figure 2 shows the simulated transmission spectrum for the slot waveguide ring resonator in the 1550 nm regime with air as the slot medium. Here it is was assumed that the effective index of the medium does not vary significantly over the wavelength range considered and can be taken constant. The design parameters for the simulated ring resonator were a Q factor of 1000 around a wavelength of 1550 nm and a free spectral range of 15 nm.

Next we simulated the same slot waveguide ring resonator structure with a diameter of 20 micrometers but with a $Si - nc/SiO_2$ material as the slot medium instead of air. Due to a change in the slot medium, the effective index of the mode in the slot waveguide would be changed and therefore the transmission resonant wavelength as well. We consider an optimized version of the slot waveguide so that the optical mode is strongly confined in the slot region. The optimized slot waveguide in a vertical configuration was obtained from (Sanchis et. al., 2007). The slot waveguide has two silicon slabs ($n_H = 3.48$) and a narrow slot region filled with a low index medium which is $Si - nc/SiO_2$ ($n_S = 1.78$), and silica ($n_C = 1.46$) material as cladding. The optimized slot waveguide dimensions are: the slab thickness (h) of 400 nm, the silicon waveguide width (w) of 220 nm, and the slot width of 100 nm (Sanchis et. al., 2007). The calculated effective index in the slot region for the waveguide dimensions considered is 2.06 (Sanchis et. al., 2007). The polarization which gives the strongest field confinement in the slot region is the x-

polarized mode or TE polarization for the considered vertical configuration of the slot waveguide (i.e. a waveguide TM mode).

The transmission spectra for the slot waveguide ring resonator with $Si - nc/SiO_2$ as the slot medium is shown in figure 3. The resonant wavelength obtained is 1.55945 micrometers. To achieve a useful extinction ratio of around 5 dB between off and on states for the switch, an effective index change (Δn_{eff}) of 9.8 $\times 10^{-4}$ is required. For slot waveguides this means a material index change in the slot region of the order of 2.33 $\times 10^{-3}$ (Barrios, 2004).

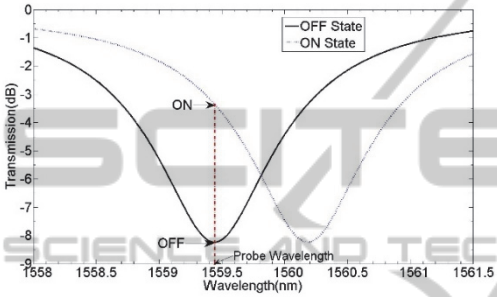

Figure 3: Kerr switch transmission spectra.

5.1 Key Performance Indicator Analysis

Here we analyse the performance of the Kerr switch in terms of key parameters for the device.

(1) Maximum modulation frequency (f_{3dB}): The 3dB modulation bandwidth for the Kerr switch is determined by the RC time constant (τ_{RC}) and the cavity photon lifetime (τ_{cav}) for the resonator structure. It can be calculated via the equation (Dong et. al., 2009)

$$f_{3dB} = \frac{1}{2\pi\sqrt{{\tau_{cav}}^2 + {\tau_{RC}}^2}} \quad (2)$$

Estimation of the capacitance of the ring waveguide structure is an electrostatic problem. Using a parallel plate capacitor formula would not account for the electrostatic energy in the fringe electric field for the structure. So we used Finite Element Methods in COMSOL as it determines the total electrostatic energy around the volume of the ring waveguide structure. The capacitance from the simulation was determined to be 16.32 fF. As expected this value is greater than the parallel plate capacitance approximation of 13.796 fF. This is due to the fringe electric field for the structure which is shown by arrows in figure 4. The relative permittivity for $Si - nc/SiO_2$ was taken as 6.2 considering a filling factor of 29 % silicon (Cada, 2011) in the simulation. For a contact resistance of 50 ohms and considering highly doped silicon slabs (carrier concentration on the order of $10^{21}/cm^3$) to ensure good ohmic contact between metal and silicon, the RC time constant is 0.816 ps. With a τ_{cav} of 0.822 ps for the ring resonator, the 3 dB modulation bandwidth for the Kerr switch is calculated to be 137.409 GHz. Such high modulation speeds have not been achieved in silicon-based electro-optic modulators. Due to the presence of high free carrier concentrations in the silicon slabs, one would have to consider associated optical losses.

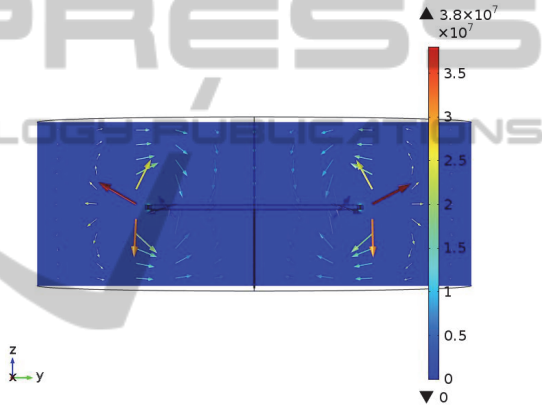

Figure 4: Electric field strength (V/m) around the ring resonator capacitor structure (YZ plane). The arrow volume indicates the electric field and the peak electric field strength is 3.718 $\times 10^7$ V/m inside the slot region.

(2) Energy/bit (fJ/bit): The modulation power consumption for a ring resonator structure of the Kerr switch would be due to charging the ring resonator which acts as a capacitor in addition to parasitic and stray capacitances. The average switching energy-per-bit (E/bit) for a lumped modulator acting as a capacitor is (Li et. al., 2013),

$$E/bit = \alpha \times CV^2 \quad (3)$$

Here C is the device capacitance; V is the applied voltage and α is the activity factor associated with the modulation encoding. Considering a pseudorandom bit sequence with $\alpha = \left(\frac{1}{4}\right)$, as the probability of a "0" to "1" transition is ¼ (Li et. al., 2013), the average switching energy-per-bit for the Kerr switch is

56.413 fJ/bit.

(3) Switching Voltage (V_{pp}): The switching voltage is determined by the required electric field to achieve the resonance shift for a useful extinction ratio. For a 5-dB extinction ratio, the material index change required in the slot region is 2.33×10^{-3}. This index change can be achieved in $Si - nc/SiO_2$ through the Kerr effect for an applied voltage of 3.718 V for a 100 nm slot width.

(4) Resonance shift efficiency (pm/V): One of the figures of merit for the ring resonator structure is the resonance shift efficiency which is the ratio of the resonant wavelength shift achieved to the applied input voltage. As discussed previously, a resonance shift of 0.75 nm is required for a 5-dB extinction ratio, and this requires a voltage of 3.718 V across the slot region. So the resonance shift efficiency in our case is 201.72 pm/V.

(5) Device footprint (μm^2): As the diameter of our chosen ring resonator structures is 20 micrometers, a substrate of 25 microns by 25 microns would be reasonable to fabricate the device. This would give the device a footprint of the order of $6.25 \times 10^2\ \mu m^2$.

(6) Working Spectrum (nm): This refers to the required operating wavelength precision for the structure. For the ring resonator considered, it is of the order of 0.1 nm. This places high demands on the fabrication accuracy for the ring resonator structure due to its narrow wavelength operating range. One would also have to consider thermal effects for the structure, which is a topic that requires further research.

The ring resonator structure considered for the Kerr switch gives excellent theoretical results for the modulation speed and resonance efficiency but with trade-offs on the extinction ratio and the Q- factor of the resonator.

6 STAGE OF RESEARCH

The different stages for the design, development, and characterization of the silicon-based Kerr switch are as follows:

1. Understanding of physical concepts involved and preliminary evaluation of performance parameters for the switch.
2. Computer aided design modeling of switch structures and simulation of the switch using numerical methods such as FDTD.
3. After useful results are obtained in stage 2, fabrication of the optimum structure for the Kerr switch.
4. Electrical characterization of the Kerr switch and comparison of experimental results and simulated results.

ACKNOWLEDGEMENTS

I would like to thank my supervisor Dr. Michael Cada for the expert guidance and the opportunity to work on this project. I also thank the ASPIRE (Advanced Science in Photonics and Innovative Research in Engineering) NSERC (Natural Science and Engineering Research Council) Program of Canada for providing financial support.

REFERENCES

Reed, G. T, Mashanovich, G., Gardes, F. Y., Thomson, D. J, 2010, *Silicon Optical Modulators,* vol. 4, Nature Photonics.

Cada, M., 2011, *Electro-Optic functionalities with Kerr Optical media*, *International Symposium on Microwave and Optical Technology*, 445- 453.

Simili, D. V., Cada, M., 2013, *Nanophotonic Silicon Electro-Optic Switch, Photonics North Conference,* Proc. Of SPIE vol. 8915 89151S1-8.

Soref, R. A., Bennett, B. R., 1987, *Electrooptical effects in Silicon*, vol. QE-23, no. 1, pp. 123-129, IEEE Journal of Quantum Electronics.

Kim, D.M., 2010, *Introductory Quantum Mechanics for Semiconductor Nanotechnology,* Wiley-VCH, Great Britain.

Saleh, B. E. A, Teich, M. C, 2007, *Fundamentals of Photonics,* John Wiley & sons, Inc., Singapore.

Xu, Q., Manipatruni, S., Scmidt, B., Shakya, J., Lipson, M., 2007, *12.5 Gbit/s carrier-injection-based silicon micro-ring silicon modulators,* vol. 15, No. 2, pp. 430-436, Optics Express.

Liu, A., Jones, R., Liao, L., Samara-Rubio, D., Rubin, D., Cohen, O., Nicolaescu, R., Paniccia, M., 2004, *A high-speed silicon optical modulator based on a metal-oxide-semiconductor capacitor,* vol. 427*,* Nature.

Liao, L., Samara-Rubio, D., Morse, M., Liu, A., Hodge, D., Rubin, D., Keil, U. D, Franck, T., 2005, *High Speed silicon Mach-Zehnder modulator,* vol. 13, no. 8, pp. 3129-3135, Optics Express.

Liao, L., Liu, A., Rubin, D., Basak, J., Chetrit, Y., Nguyen H., Cohen, R., Izakhy, N., Paniccia, M., 2007, *40 Gbit/s silicon optical modulator for high speed applications,* vol. 43, no. 22, Electronics Letters.

Cada, M., 2008, *Research Report on Electro-Optic Materials*, Nanophotonic Technology Center, Polytechnic University of Valencia, Spain.

R. W. Boyd, 2008, *Nonlinear Optics*, Elsevier, Amsterdam, 3rd edition.

Cada, M., Qasymeh, M., and Pistora, J., 2008, *Electrically and optically controlled cross-polarized wave conversion*, vol. 16, no. 5, pp. 3083-3100, Optics Express.

Martinez, A., Blasco, J., Sanchis, P., Galan, J.,V., Garcia-Ruperez, J., Jordana, E., Gautier, P., Lebour, Y.,Hernanadez, S., Daldosso, N., Garrido, B., Fedili, J.,M., Pavesi, L. and Marti, J., 2010, *Ultrafast All-Optical Switching in a Silicon-Nanocrystal-Based Silicon Slot Waveguide at Telecom Wavelengths*, 10, pp.1506-1511, Nano Letters.

Xu, Q., Almeida, V., R., Panepucci, R., R. and Lipson, M., 2004, *Experimental demonstration of guiding and confining light in nanometer-size low-refractive-index material*, vol. 29, no. 14, pp. 1626-1628 Optics Letters.

Sanchis, P., Martinez, A., 2007, *Design of Silicon-Based Slot Waveguide Configurations for Optimum Nonlinear Performance,* vol. 25, no. 5, Journal of Lightwave Technology.

Barrios, C. A., 2004, *High-performance all-optical silicon microswitch,* vol. 40, no. 14, Electronics Letters.

Dong, P., Liao, S., Feng, D., Liang, H., Zheng, D., Shafiiha, R., Kung, C., Quian W., Li, G., Zheng, X., Krishnamoorthy, A. V., Asghari, M., 2009, *Low V_{pp}, ultralow-energy, compact, high-speed silicon electro-optic modulator,* vol. 17, no. 25, Optics Express.

Li, G., Krishnamoorthy, A. V, Shubin, I., Yao, J., Luo, Y., Thacker, H., Zheng, X., Raj, K., Cunningham, J. E., 2013, *Ring Resonator Modulators in Silicon for Interchip Photonic Links,* vol. 19, no. 6, IEEE journal of selected topics in Quantum Electronics.